Supporting Information

Smaers et al. 10.1073/pnas.1212181109

SI Text

Models of Evolution: Adaptive Peak, Brownian Motion, and Ornstein–Uhlenbeck Model. To reconstruct evolutionary history based on extant data and a phylogenetic tree, models of evolution are used that dictate the principles by which one may "count back in time" along the branches of the tree (1). These models commonly originate in physics, where they are used to describe the movement of particles in space (2–5). Applied to comparative biology, these models set out a list of rules that describe how to use extant trait variation and the phylogenetic relatedness between the species in the sample to infer what is the most plausible set of changes that underlies extant variation (i.e., how traits "move" through phylogenetic space) (6, 7).

The most commonly used model [Brownian motion (BM)] dictates that (*i*) rates of change are constant throughout time and along all branches and (*ii*) the probability of trait change is independent of both prior and current character states and of changes elsewhere in the tree (8). The constancy of rate assumption has received much criticism in particular because it is inappropriate to model selection (9, 10), which inherently assumes differential change in time and along different branches. To overcome this limitation, additional parameters can be included to allow BM to deviate from a null model of "constancy of rate" (7, 11, 12). The use of an Ornstein–Uhlenbeck (OU) model (12, 13), for example, can be interpreted as a BM model that allows for differential rates of change along different branches by including "adaptive optima" at certain topological locations in the phylogenetic tree. Additional parameterization is, however, generally considered undesirable because it necessarily involves increased reliance on a priori assumptions (14).

The adaptive peak (AP) model of evolution, particularly its formalization by the method of independent evolution (IE), moves away from using constancy of rate as a null model. The AP model assumes that rates of change are inherently different for each branch in the phylogenetic tree as APs wander through phylogenetic space (15). The IE formalization of the AP model further allows for the incorporation of BM and OU assumptions by collapsing its algorithms accordingly under relevant conditions (16). In other words, when extant variation gives evidence of BM- or OU-like evolution, IE will recognize it as such without the need to include additional parameters. IE thus overcomes the problem of additional parameterization by relying only on extant variation and a phylogenetic tree; no extra parameters are needed to infer branch-specific rates of change for all branches of a phylogenetic tree.

Example: Reconstructing the Ancestral Brain Size of Chimpanzees and Humans. When reconstructing the ancestral brain size of the most recent common ancestor of humans and chimpanzees, traditional BM methods estimate this value around the arithmetic mean of humans and chimpanzees at between 700 cc and 850 cc, assuming a constant rate of change across time, and thus equal evolutionary rates in sister species with equal branch lengths. We know from the fossil record, however, that the brain size of this ancestor is more likely to be around the chimpanzee's value (~380 cc), implying that the chimpanzee lineage did not increase much (or even decreased) in brain size since its most recent common ancestor with humans [*Australopithecus afarensis*, with a brain size of ~433 cc (17), is the oldest uncontroversial hominin for which brain size can be reliably inferred]. Thus, the inference of BM methods of equal change along sister branches with equal branch lengths cannot be considered valid in this example. Moreover, differential patterns of change between sister species is considered a fundamental characteristic of selection, making the BM model inappropriate to model selection (1, 9, 10, 12, 15, 18, 19).

The advantage of the AP model, on which the IE method is based, is that it allows inferring differential change in sister species by recognizing that ancestral values are likely to be close to the values of other species that are phylogenetically closely related to them. In the case of the human-chimpanzee most recent common ancestor, the IE method looks toward values of the bonobo (~350 cc), gorilla (~500 cc), and orangutan (~400 cc), and parsimoniously infers the human-*Pan* ancestral value at around 400 cc (at 403 cc, node 10 in Fig. S1 and Table S1), resulting in the inference of a low evolutionary rate of brain size in the chimpanzee ancestral lineage and a high rate in the human ancestral lineage (Fig. S1 and Table S1), in line with the fossil evidence. By allowing for differential rates of evolution in separate branches of sister species (BM assumes equal rates), the IE method is able to assess branch-specific rates of evolution, thereby increasing the resolution at which we can estimate ancestral values based on extant variation.

1. Harvey PH, Pagel M (1991) *The Comparative Method in Evolutionary Biology* (Oxford Univ Press, New York).
2. Brown R (1828) A brief description of microscopical observations made in the months of June, July and August 1827, on the particles contained in the pollen of plants; and on the general existence of active molecules in organic and inorganic bodies. *Ann Phys* 14:294–313.
3. Uhlenbeck GF, Ornstein LS (1930) On the theory of the Brownian motion. *Phys Rev* 36: 823–841.
4. Einstein A (1956) *Investigations on the Theory of the Brownian Movement* (Dover, New York).
5. Einstein A (1905) Über die von der molekularkinetischen Theorie der Wärme geforderte Bewegung von in ruhenden Flüssigkeiten suspendierten Teilchen. *Annalen der physik* 322(8):549–560.
6. Edwards AWF, Cavalli-Sforza LL (1964) Reconstruction of evolutionary trees. *Phenetic and Phylogenetic Classification*, eds Heywood VH, McNeill J (Systematics Association, London), pp 67–76.
7. Pagel M (1999) Inferring the historical patterns of biological evolution. *Nature* 401: 877–884.
8. Webster AJ, Purvis A (2002) Ancestral states and evolutionary rates of continuous characters. *Morphology, Shape and Phylogeny*, eds MacLeod N, Porey P (Taylor and Francis, London), pp 247–268.
9. Westoby M, Leishman MR, Lord JM (1995) On misinterpreting the phylogenetic correction. *J Ecol* 83:531–534.
10. Price T (1997) Correlated evolution and independent contrasts. *Philos Trans R Soc Lond B Biol Sci* 352:519–529.
11. Venditti C, Meade A, Pagel M (2011) Multiple routes to mammalian diversity. *Nature* 479:393–396.
12. Butler MA, King AA (2004) Phylogenetic comparative analysis: A modeling approach for adaptive evolution. *Am Nat* 164:683–695.
13. Hansen TF (1997) Stabilizing selection and the comparative analysis of adaptation. *Evolution* 51:1341–1351.
14. Akaike H (1974) A new look at the statistical model identification. *IEEE Transactions on Automatic Control* 19:716–723.
15. Felsenstein J (1988) Phylogenies and quantitative characters. *Annu Rev Ecol Syst* 19: 445–471.
16. Smaers JB, Vinicius L (2009) Inferring macro-evolutionary patterns using an adaptive peak model of evolution. *Evol Ecol Res* 11:991–1015.
17. Fleagle JG (1999) *Primate Adaptation and evolution* (Academic Press, San Diego, CA).
18. Harvey PH, Rambaut A (2000) Comparative analyses for adaptive radiations. *Philos Trans R Soc Lond B Biol Sci* 355:1599–1605.
19. Hansen TF, Orzack SH (2005) Assessing current adaptation and phylogenetic inertia as explanations of trait evolution: The need for controlled comparisons. *Evolution* 59: 2063–2072.

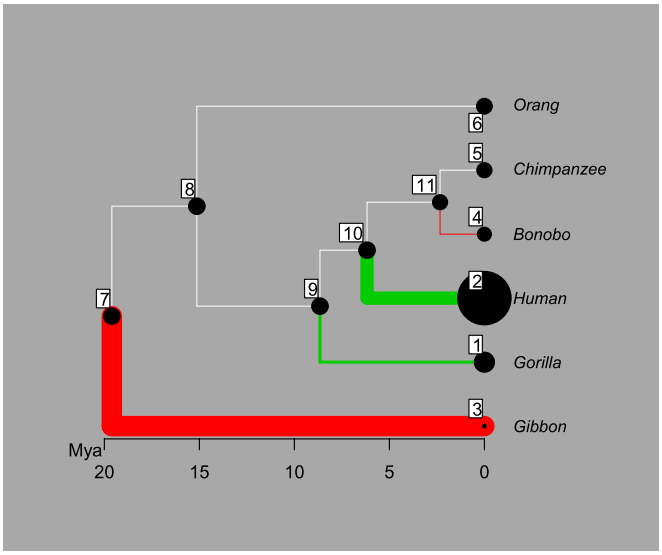

Fig. S1. Graphic representation of the reconstruction of brain size evolution in apes. Label size represents brain size; green and red branches indicate positive (trait increase) and negative (trait decrease) rates, respectively; white branches indicate branches with low trait change (rate close to 0); and branch width indicates the value of the rate (high rate is thick branch, low rate is thin branch).

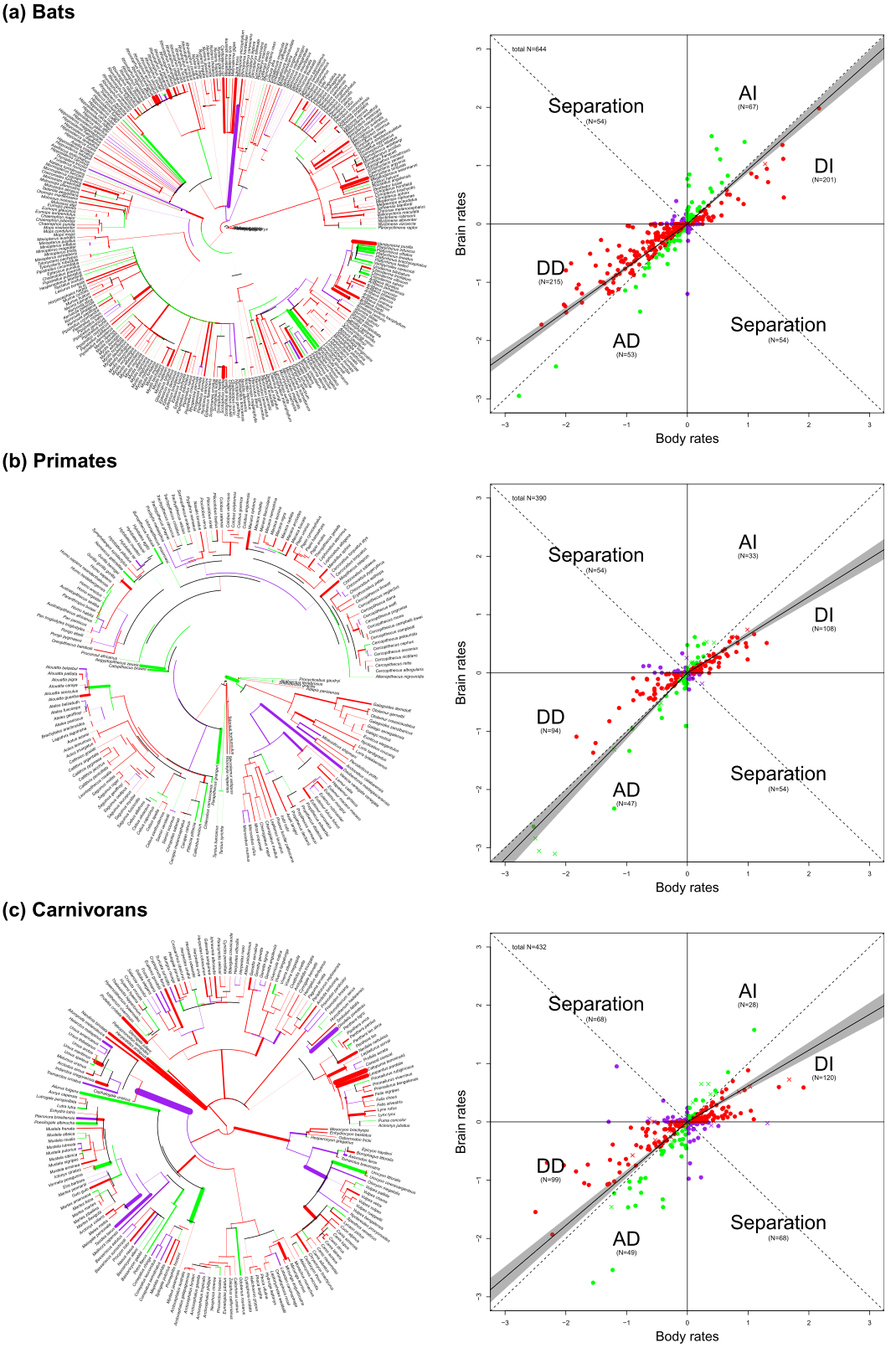

Fig. S2. High-resolution image of Fig. 4. AI, accelerated increase; AD, accelerated decrease; DD, decelerated decrease; DI, decelerated increase.

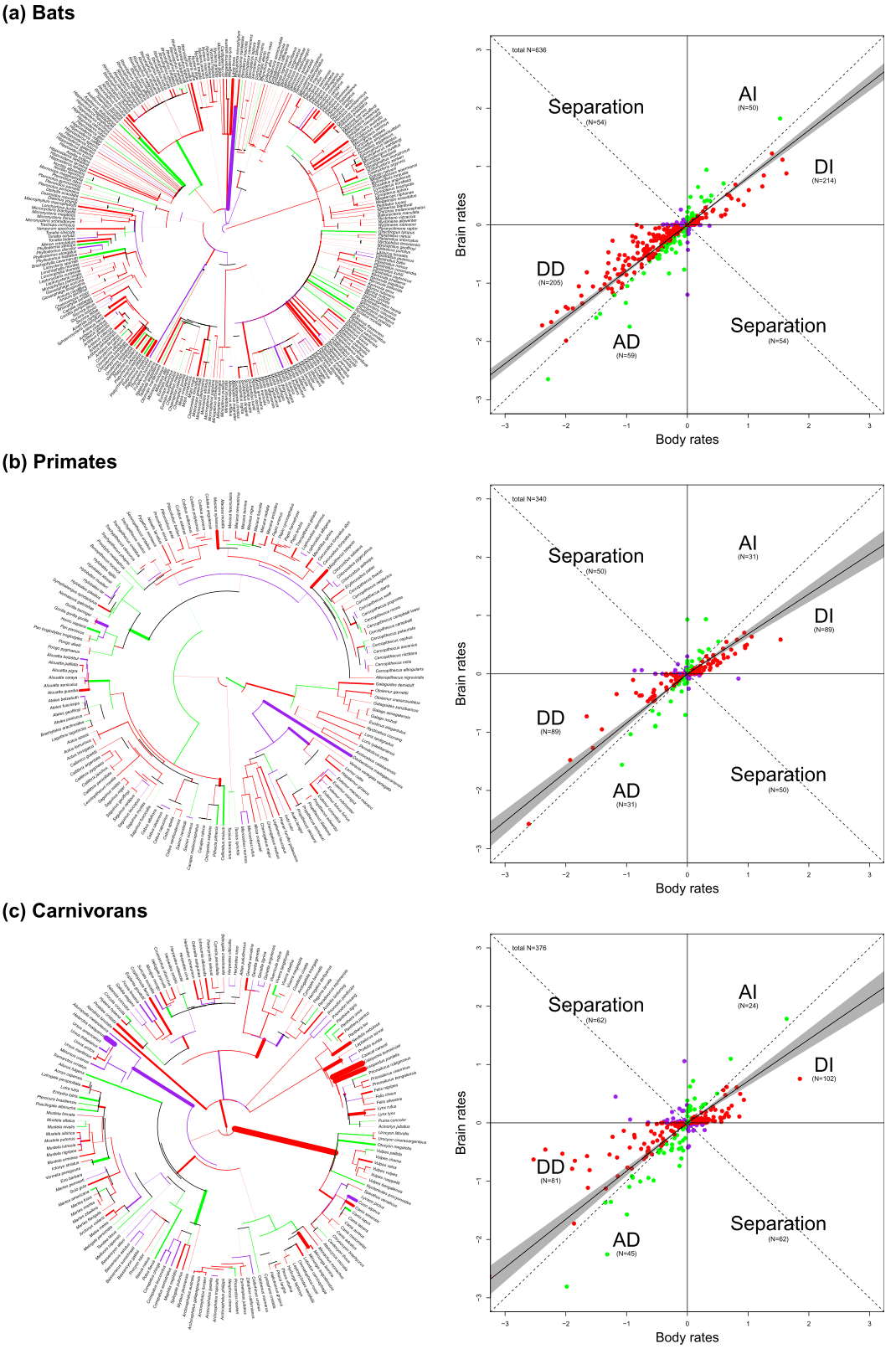

Fig. S3. Analysis and representations as in Fig. 4 based on values of extant species only. AI, accelerated increase; AD, accelerated decrease; DD, decelerated decrease; DI, decelerated increase.

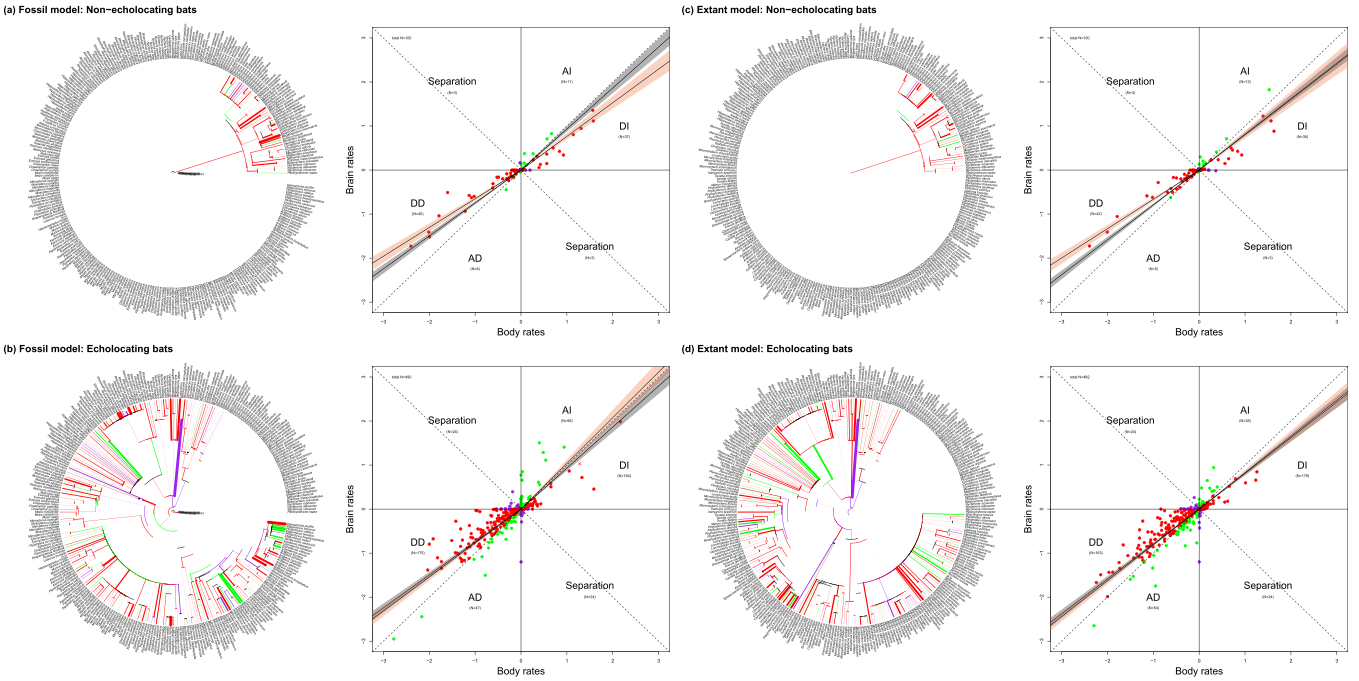

Fig. S4. Analysis and representations as in Fig. 4. Results for nonecholocating bats (*A* and *C*) and echolocating bats (*B* and *D*) are displayed. The fossil model (*A* and *B*) and extant model (*C* and *D*) are shown. AI, accelerated increase; AD, accelerated decrease; DD, decelerated decrease; DI, decelerated increase.

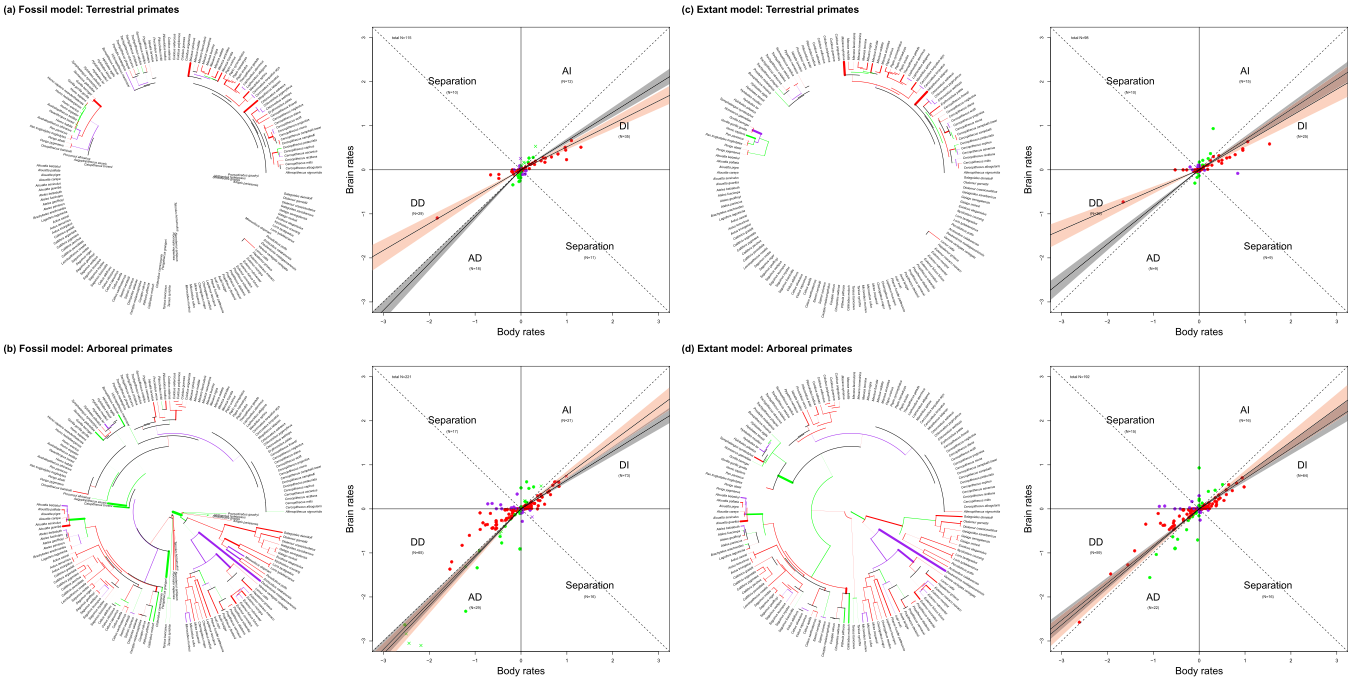

Fig. S5. Analysis and representations as in Fig. 4. Results for terrestrial primates (*A* and *D*) and arboreal primates (*B* and *D*) are displayed. The fossil model (*A* and *B*) and extant model (*C* and *D*) are shown. AI, accelerated increase; AD, accelerated decrease; DD, decelerated decrease; DI, decelerated increase.

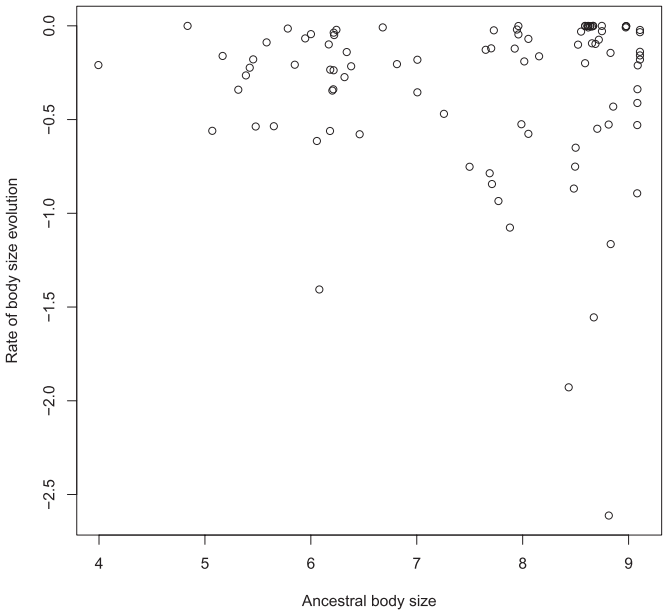

Fig. S6. Plot of body size rates for lineages that indicate a decrease in body size relative to the inferred ancestral body size of their lineage.

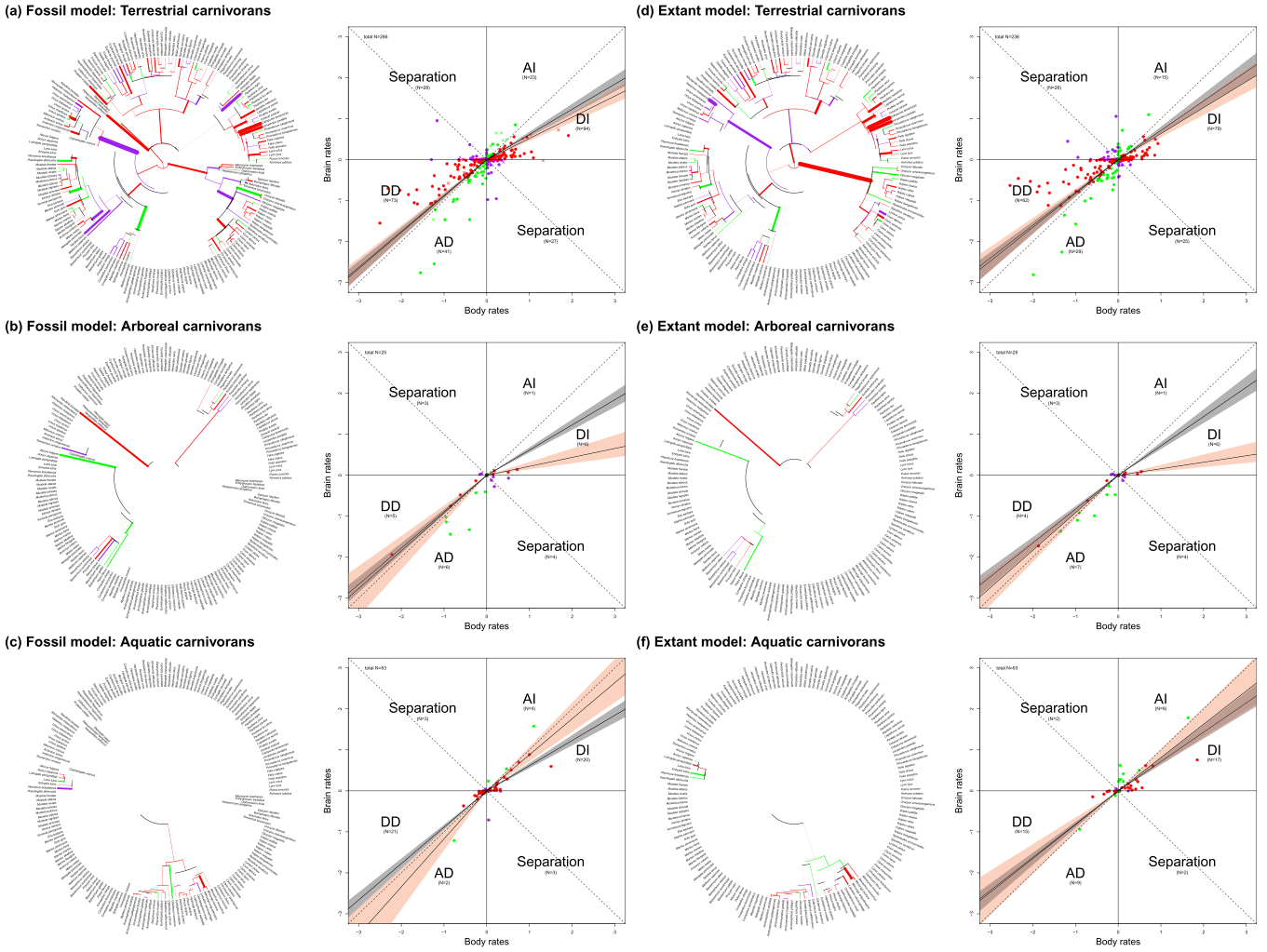

Fig. S7. Analysis and representations as in Fig. 4. Results for terrestrial carnivorans (*A* and *D*), arboreal carnivorans (*B* and *E*), and aquatic carnivorans (*C* and *F*) are displayed. The fossil model (*A*–*C*) and extant model (*D*–*F*) are shown. AI, accelerated increase; AD, accelerated decrease; DD, decelerated decrease; DI, decelerated increase.

Table S1. Results of the reconstruction of brain size evolution in apes

Ancestral node	Descendant node	Ancestral value	Descendant value	Rate
7	3	401.03	90.17	−1.994
7	8	401.03	403.65	0.017
8	9	403.65	403.66	0.000
9	1	403.66	490.84	0.303
9	10	403.66	403.63	0.000
10	2	403.63	1302.01	1.296
10	11	403.63	368.34	−0.051
11	4	368.34	341.29	−0.076
11	5	368.34	368.35	0.000
8	6	403.65	383.44	−0.072

Ancestral and descendant node numbers correspond to those in Fig. S1. Ancestral and descendant value indicate brain mass (gr).

Table S2. Results of the reduced major axis analysis using residuals orthogonal to the isometric line

			1,000 replications			
Reduced major axis			Decrease	Increase	Decrease	Increase
Extants	Bats	All	0.76–0.83	0.77–0.86	0.73–0.78	0.78–0.88
		Nonecholocating	0.63–0.71	0.72–0.89		
		Echolocating	0.78–0.85	0.76–0.89		
	Primates	All	0.78–0.91	0.62–0.76	0.78–0.91	0.61–0.76
		Terrestrial	0.38–0.54	0.51–0.73		
		Arboreal	0.80–0.96	0.67–0.87		
	Carnivorans	All	0.75–0.91	0.64–0.80	0.74–0.89	0.66–0.84
		Terrestrial	0.72–0.91	0.55–0.74		
		Arboreal	0.79–1.02	0.10–0.25		
		Aquatic	0.65–1.01	0.65–1.02		
			Decrease	Increase		
Fossils	Bats	All	0.72–0.78	0.87–0.99		
		Nonecholocating	0.61–0.70	0.70–0.84		
		Echolocating	0.73–0.81	0.96–1.12		
	Primates	All	0.99–1.14	0.60–0.71		
		Terrestrial	0.53–0.71	0.46–0.59		
		Arboreal	1.02–1.19	0.69–0.85		
	Carnivorans	All	0.83–0.95	0.55–0.68		
		Terrestrial	0.81–0.97	0.46–0.59		
		Arboreal	0.74–1.05	0.13–0.28		
		Aquatic	0.95–1.45	0.72–1.08		

Results of the reduced major axis analysis using residuals orthogonal to the isometric line (as in Fig. 2) are shown. Analyses were performed separately for all increase branches (accelerated and decelerated increase) and for all decrease branches (accelerated and decelerated decrease). Results of the fossil and extant models for all subgroups of all orders are presented. For the extant model, an additional analysis was performed to quantify the effect of randomly resolving polytomies [more information is provided in *Materials and Methods* (*Analysis*)].

Table S3. Comparison between different orders within evolutionary scenarios

	Fossil models						Extant models					
		Magnitude			Variance			Magnitude			Variance	
	P.adj	Mean (x)	Mean (y)	*P*	*F*	df	*P*.adj	Mean (x)	Mean (y)	*P*	*F*	df
AI				0.558	0.587	125				0.068	2.768	102
Primates v bats	0.530	0.058	0.088				0.879	0.073	0.060			
Primates v carnivorans	0.874	0.058	0.075				0.204	0.073	0.127			
Bats v carnivorans	0.894	0.088	0.075				0.057	0.060	0.127			
DD				0.002	6.135	405				0.000	10.042	372
Primates v bats	0.072	0.096	0.143				0.158	0.095	0.138			
Primates v carnivorans	0.001	0.096	0.183				0.000	0.095	0.218			
Bats v carnivorans	0.138	0.143	0.183				0.002	0.138	0.218			
DI				0.000	23.323	426				0.000	25.249	402
Primates v bats	0.008	−0.087	−0.044				0.000	−0.095	−0.041			
Primates v carnivorans	0.004	−0.087	−0.138				0.162	−0.095	−0.122			
Bats v carnivorans	0.000	−0.044	−0.138				0.000	−0.041	−0.122			
AD				0.005	5.547	146				0.069	2.731	132
Primates v bats	0.159	−0.120	−0.055				0.953	−0.076	−0.067			
Primates v carnivorans	0.339	−0.120	−0.171				0.237	−0.076	−0.126			
Bats v carnivorans	0.003	−0.055	−0.171				0.066	−0.067	−0.126			

The results indicate a variance analysis and *t* test of positive orthogonal residuals relative to the isometric line between different mammalian orders for the four evolutionary scenarios. P.adj, adjusted *P* values using Tukey's honestly significant difference.

Table S4. Comparison within different orders between evolutionary scenarios

	Fossil models				Extant models			
	P	*t*	Mean (*x*)	Mean (*y*)	*P*	*t*	Mean (*x*)	Mean (*y*)
AI vs. DI								
Bats	0.037	2.119	0.088	0.044	0.185	1.340	0.060	0.041
Primates	0.118	−1.585	0.058	0.087	0.410	−0.832	0.073	0.095
Carnivorans	0.009	−2.690	0.075	0.138	0.879	0.153	0.127	0.122
DD vs. AD								
Bats	0.000	5.341	0.143	0.055	0.000	3.943	0.138	0.067
Primates	0.433	−0.789	0.096	0.120	0.454	0.754	0.095	0.076
Carnivorans	0.745	0.327	0.183	0.171	0.022	2.312	0.218	0.126

P values from a *t* test between absolute values of the positive and negative orthogonal residuals relative to the isometric line within all three mammalian orders. AI, accelerated increase; AD, accelerated decrease; DD, decelerated decrease; DI, decelerated increase.

Table S5. List of all fossil information used in the analyses

Species	Brain, g	Body, g	Estimated divergence from sister lineage, Mya	Estimated last occurrence, Mya
Bats				
Icaronycteris	334	13	65	63
Archaeonycteris	503	23	58	57
Paleochiropteryx	300	11	57	56
Hassianycteris	883	53	57	54
Primates				
Homo neanderthalensis	1,582	65,000	0.56	0.03
Homo heidelbergensis	1,118	62,000	0.7	0.3
Homo erectus	951	57,000	1.8	0.3
Homo ergaster	802	58,000	1.9	1.5
Australopithecus sediba	420	35,999	2	1.9
Paranthropus boisei	486	44,000	2.3	1.4
Homo habilis	522	34,000	2.4	1.6
Australopithecus africanus	434	36,000	3	2
Proconsul africanus	161	10,500	29	19
Oreopithecus bambolii	383	30,000	16	6
Victoriapithecus macinnesi	53	4,500	23	10.5
Aegyptopithecus zeuxis	34	6,710	42	30
Catopithecus browni	3	900	44	34
Parapithecus grangeri	12	1,800	49	39
Chilecebus carrascoenis	8	582	23	20
Mioeuoticus shipmani	8	1,280	30	18
Adapis parisiensis	9	2,350	67	34
Smilodectes gracilis	10	1,960	66.9	48
Pronycticebus gaudryi	5	1,220	66	38
Notharctus tenebrosus	11	1,990	50	47
Rooneyia viejaensis	8	782	71	35
Necrolemur antiquus	4	233	69.9	35
Tetonius homunculus	2	74	61	55
Carnivorans				
Aelurodon ferox	134	35,750	16	12
Borophagus littoralis	127	32,040	12	9
Epicyon haydeni	131	71,860	12	7
Tomarctus brevirostris	51	19,390	27	15
Canis dirus	178	63,370	1	0.01
Enhydrocyon basilatus	74	28,990	29	21
Hesperocyon gregarius	15	2,300	37	29
Mesocyon brachyops	39	7,290	28.5	21
Osbornodon fricki	101	38,310	30	17
Promephitis hootoni	12	1,530	17	7.1
Cephalogale ursinus	184	26,170	23.8	22.8
Arctodus simus	683	32,8470	3	0.01
Indarctos oregonensis	647	545,490	10.3	5.3
Ursus spelaeus	653	300,000	1.6	0.02
Herpestides antiquus	26	4,000	53.1	20
Paleoprionodon lamandini	9	1,970	30	20
Stenogale julieni	10	2,140	30	20
Dinofelis piveteaui	154	259,820	18.3	1.2
Homotherium hadarensis	212	106,470	14	1.8
Homotherium serus	332	150,000	6	0.01
Panthera leo atrox	460	206,380	1.8	0.01
Smilodon fatalis	346	225,600	16	0.01
Hyaenictitherium hyaenoides	91	23,160	13	7
Ictitherium viverrinum	61	18,000	12.5	5.3
Thalassictis hipparionum	78	18,960	14	5

References for fossil and extant species data are provided (1–12).

1. Finarelli JA, Flynn JJ (2009) Brain-size evolution and sociality in Carnivora. *Proc Natl Acad Sci USA* 106:9345–9349.
2. Kappelman J (1996) The evolution of body mass and relative brain size in fossil hominids. *J Hum Evol* 30:243–276.
3. Strait SG (2001) Dietary reconstruction of small-bodied omomyoid primates. *J Vertebr Paleontol* 21:322–334.
4. Parr WCH, Chatterjee HJ, Soligo C (2011) Inter- and intra-specific scaling of articular surface areas in the hominoid talus. *J Anat* 218:386–401.
5. Montgomery SH, Capellini I, Barton RA, Mundy NI (2010) Reconstructing the ups and downs of primate brain evolution: Implications for adaptive hypotheses and Homo floresiensis. *BMC Biol* 8:9.
6. Baron G, Stephan H, Frahm HD (1996) *Comparative Neurobiology in Chiroptera* (Birkhäuser, Basel), 1st Ed.

7. Simons EL (2001) The cranium of Parapithecus grangeri, an Egyptian Oligocene anthropoidean primate. *Proc Natl Acad Sci USA* 98:7892–7897.
8. Kirk EC, Simons EL (2001) Diets of fossil primates from the Fayum Depression of Egypt: A quantitative analysis of molar shearing. *J Hum Evol* 40:203–229.
9. Sears KE, Finarelli JA, Flynn JJ, Wyss AR (2008) Estimating body mass in New World "monkeys" (Platyrrhini, Primates), with a consideration of the Miocene platyrrhine, Chilecebus carrascoensis. *Am Mus Novit* 3617:1–29.
10. Norberg UM (1987) Wing form and flight modes in bats. In: *Recent Advances in the Study of Bats*, eds Fenton MB, Racey PA, Rayner JMV (Cambridge University Press, Cambridge), pp 43–56.
11. Isler K, et al. (2008) Endocranial volumes of primate species: Scaling analyses using a comprehensive and reliable data set. *J Hum Evol* 55:967–978.
12. Martin RD (1990) *Primate Origins and Evolution: A Phylogenetic Reconstruction* (Chapman and Hall, London).